# Superoscillations Deliver Superspectroscopy

Gerard McCaul,* Peisong Peng,† Monica Ortiz Martinez,‡ Dusty R. Lindberg,§
Diyar Talbayev,‖ and Denys I. Bondar¶
*Tulane University, New Orleans, Louisiana 70118, USA*

(Received 3 March 2023; revised 12 September 2023; accepted 15 September 2023; published 12 October 2023)

In ordinary circumstances the highest frequency present in a wave is the highest frequency in its Fourier decomposition. It is however possible for there to be a spatial or temporal region where the wave locally oscillates at a still greater frequency in a phenomenon known as superoscillation. Superoscillations find application in wide range of disciplines, but at present their generation is based upon constructive approaches that are difficult to implement. Here, we address this, exploiting the fact that superoscillations are a product of destructive interference to produce a prescription for generating superoscillations from the superposition of arbitrary waveforms. As a first test of the technique, we use it to combine four quasisinusoidal THz waveforms to produce THz optical superoscillations for the first time. The ability to generate superoscillations in this manner has potential application in a wide range of fields, which we demonstrate with a method we term "superspectroscopy." This employs the generated superoscillations to obtain an observed enhancement of almost an order of magnitude in the spectroscopic sensitivity to materials whose resonance lies outside the range of the component waveform frequencies.

DOI: 10.1103/PhysRevLett.131.153803

*Introduction.*—In the modern era, light has assumed a role of central importance in both industry and research. It is not only a subject of fundamental study, but a tool for the manipulation of matter [1–8], a medium of computation [9–14], and a probe of physical systems. It is often assumed that the ultimate limitations of light for imaging and other optical experimentation correspond to the highest frequency in its Fourier decomposition. In some cases however, it is possible to construct a *superoscillation* (SO), a band-limited signal that has a temporal or spatial region in which it oscillates at a frequency faster than its fastest Fourier component [15].

The term "superoscillation" was first coined by Michael Berry [15–17] in reference to work by Aharonov, Bergman, and Lebowitz [18]. Today, superoscillations constitute a rapidly developing field of study in both mathematics [19,20] and physics [21,22]. The main hinderance to the application of superoscillations has been their minute intensity as compared to the full waveform, but advances in the general sensitivity of measurements mean that the relative amplitudes of superoscillations are no longer an impediment to their study and application [15]. These applications cover a broad range of topics, including optical metrology [23], super-resolution [24–26], supertransmission [27–29], and free-space plasmonics [30].

In the spatial domain, there have been a number of experimental observations of superoscillations [17,31–33] that extend even into the THz optical frequency range and allow for imaging below the diffraction limit [34]. This raises the tantalizing possibility that nanoscale imaging with visible light may be made possible by superoscillation [35].

In the temporal domain, radio frequency superoscillations have been employed [29,36,37], while THz acoustic superoscillations have been observed in superlattices [38]. The envelopes of laser pulses have also been manipulated to display superoscillatory behavior (relative to the envelope frequency) [39–41]. To this point however, there has been no direct observation of a THz time domain optical superoscillation relative to the carrier frequency. Much like in the spatial domain, temporal superoscillations have tremendous potential to broaden the domain of useful operation for current technology. For example, the supertransmissive property of superoscillations [27] also means that they can be used to transmit light through media at frequencies that would ordinarily be absorbed. This has the potential to allow for the probing of materials in a range at which they would ordinarily be optically opaque. Another context in which time domain optical superoscillations might usefully be employed are Aharonov-type pulse slicing experiments [42–45]. Performing this slicing in the superoscillatory region of a pulse could be used to generate highly energetic "gamma ray" photons.

At present, the prescriptions for directly constructing superoscillations (as opposed to achieving them via the design of lenses [46] or filters [25]) have been based on the analysis of band-limited functions, but transitioning to experimentally viable approximations of such functions is fraught with difficulties [47–49]. Despite the sensitivity of purposely constructed superoscillations, there has been a preponderance of "accidental" superoscillations observed both in random functions [16] and more structured fields [50,51]. While a number of methods for the synthesis of THz waveforms have been developed [52–55], we present here a simple heuristic technique aimed directly at the generation of superoscillations, based on the observation that a superoscillation can be interpreted as product of destructive interference within a given observational window.

In addition to the generation of superoscillations, we experimentally demonstrate that these fields can be used in a novel technique for off-resonance sensing and detection, which we term "superspectroscopy." This method employs superoscillatory fields to amplify time-local differences between similar optical systems, and enhance one's ability to distinguish between them. Not only does this extend the range of spectroscopically accessible frequencies by currently available light sources, but when combined with supertransmissive properties has the potential to enable detection and sensing even when transmitting through highly absorbent media.

*Superoscillations.*—The phenomenon of superoscillations has typically been studied in the context of the function [16,26]

$$F_n(a,t) = \left[\cos\frac{t}{n} + ia\sin\frac{t}{n}\right]^n. \tag{1}$$

The behavior of this function for small $t$ (or equivalently large $n$) can be obtained by Taylor expanding to first order:

$$F_n(a,t) \approx \left(1 + ia\frac{t}{n}\right)^n \approx \mathrm{e}^{iat}. \tag{2}$$

When $a = 1$ this expression is exact for any $n$, but in the case of $a > 1$, it produces the counterintuitive behavior that $F_n(a,t)$ oscillates faster than its highest frequency Fourier component, $e^{it}$. To show this, let us re-express Eq. (1) as a Fourier series. The most direct route to achieving this is to express the trigonometric functions as exponentials before performing a binomial expansion. This leads directly to the Fourier expansion of $F_n(a,t)$:

$$F_n(a,t) = \sum_{j=0}^{n} A_j \mathrm{e}^{i\omega_j t}, \tag{3}$$

$$A_j = \frac{1}{2^n}\binom{n}{j}(1+a)^{n-j}(1-a)^j, \tag{4}$$

$$\omega_j = 1 - 2\frac{j}{n}. \tag{5}$$

Regardless of the value of $a$ chosen, the highest frequency in the Fourier decomposition will be $k_0 = 1$. Hence, for $a > 1$, the function close to the origin will "superoscillate" at a frequency greater than its largest Fourier component. This is illustrated in Fig. 1 (top panel), where the frequency of the superoscillation relative to its largest Fourier component increases with $a$.

A function of the type described by Eq. (1) is far from the only way to obtain a superoscillation however. Careful examination of the secondary properties $F_n(a,t)$ can be used to formulate an alternative prescription for generating superoscillations. Here, we focus on the fact that superoscillations occur in the region where $|F_n(a,t)|^2$ is minimized, as shown by Fig. 1 (bottom panel). This phenomenon can be understood heuristically by noting that the magnitude

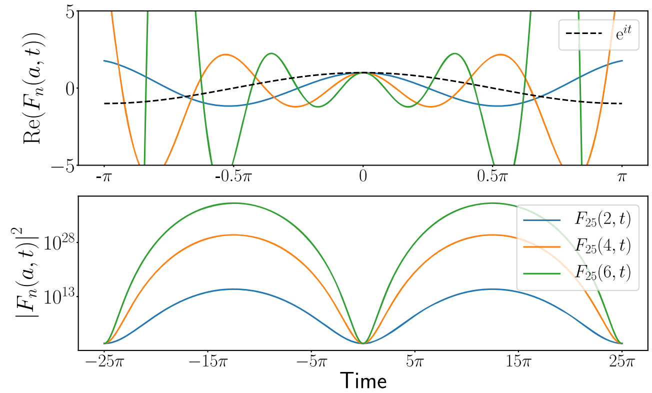


FIG. 1. Comparison of superoscillating functions (top panel) to their intensities (bottom panel). Comparison between the two panels readily demonstrates that the region where the magnitude $|F_n(a,t)|^2$ is minimized corresponds to a superoscillatory window where the function oscillates faster than its greatest Fourier component $k_0 = 1$ (shown as dashed line). The precise frequency achieved by the superoscillation is a function of the parameter $a$.

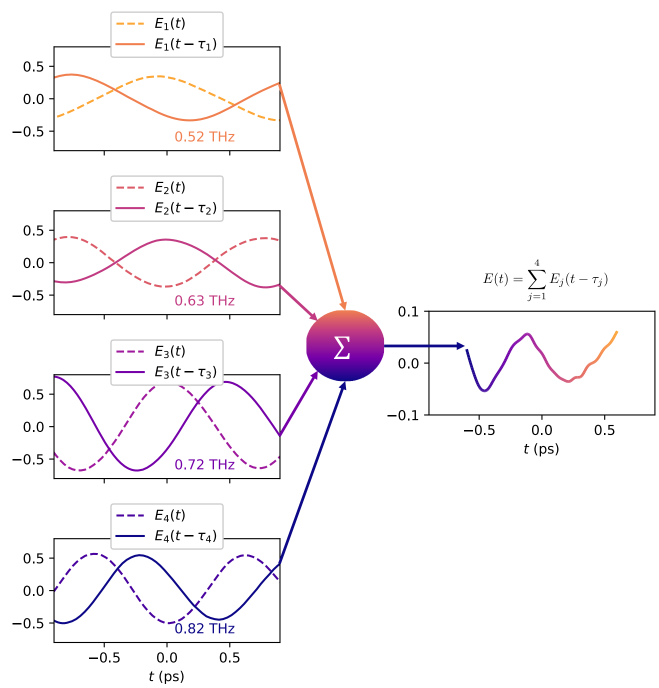


FIG. 2. Left side: experimentally measured near-sinusoidal THz waveforms before (dashed lines) and after (solid lines) implementing the time delays $\tau_j$ found by minimizing the objective function, Eq. (7). Right side: the measured superoscillation formed by the time-shifted waveforms in the window of minimization $t \in [-T_{\mathrm{SO}}, T_{\mathrm{SO}}]$.

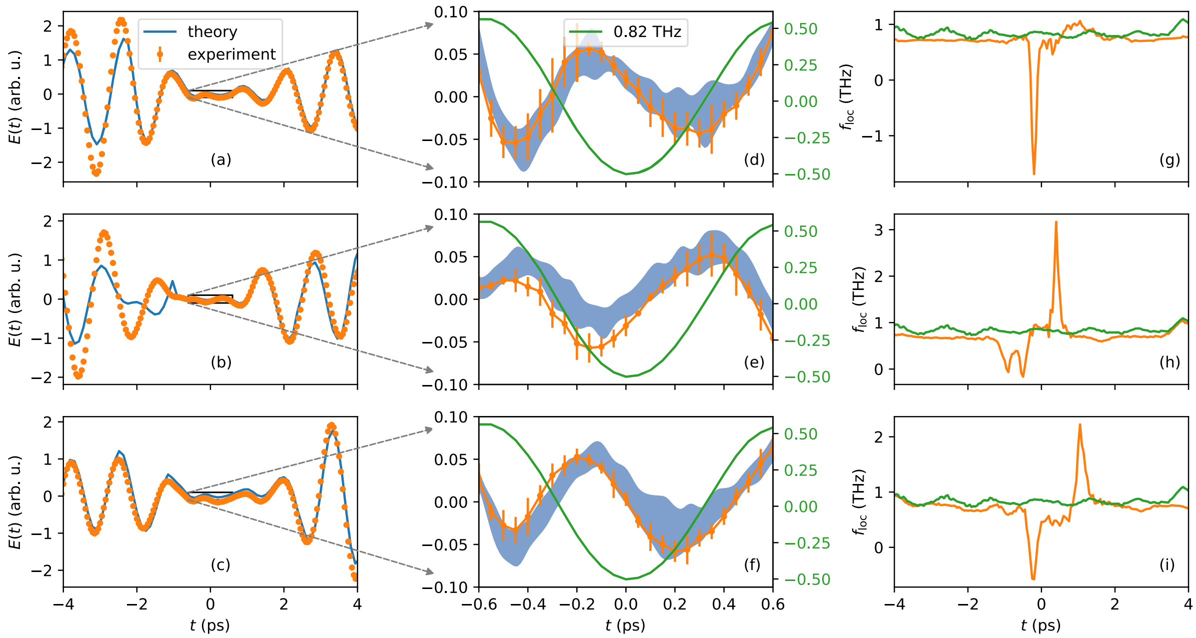


FIG. 3. Three example superoscillations obtained via the minimization of Eq. (7). Left column [(a)–(c)] shows both the predicted and observed field over the full measurement window. The middle panels [(d)–(f)] highlight the window in which the superoscillation occurs, with comparison to the highest frequency component waveform. The experimental data is in excellent agreement with the theoretical 95% confidence limit (shaded blue area). The right column [(g)–(i)] plots the local frequencies of both the total waveform and its highest frequency component. Outside the window of minimization these are roughly equivalent, but within this window the combined waveform's local frequency increases sharply compared to that of the highest frequency component.

of the superoscillation will be of order 1 by Eq. (2). Examination of the Fourier components via Eq. (4) however shows individual frequencies may have much larger amplitudes. The size of these components can only be reconciled with the superoscillation if there is near total cancellation of the individual field components around $t = 0$. This means that *superoscillations are a product of destructive interference*. This fact allows us to use the proxy of destructive interference as a figure of merit for the construction of superoscillations.

Let us now apply this logic to the problem of generating a superoscillating optical field $E(t)$ using a set of experimentally accessible, time-limited $E_j(t)$ waveforms with different central frequencies $f_j$. Each waveform has an amplitude $a_j$ and time delay $\tau_j$ such that the total field is given via

$$E(t) = \sum_{j=1}^{N} a_j E_j(t - \tau_j). \tag{6}$$

We wish to select our parameters such that the intensity of this waveform is minimized over some time window $t \in [-T_{\mathrm{SO}}, T_{\mathrm{SO}}]$, which we shall refer to as the region of minimization. This immediately presents two difficulties if one varies amplitudes. First, in order to avoid the trivial solution $a_j = 0$, it is necessary to condition any minimization to avoid this outcome. Moreover, amplitude modulation is guaranteed to reduce the integrated intensity of the full waveform, making experimental detection more challenging.

For this reason, we consider only variations of the time delays $\tau_j$ when minimizing intensity within a given temporal region (i.e., setting $a_j = 1$). Explicitly, we wish to minimize the objective function

$$I(\{\tau_j\}) = \int_{-T_{\mathrm{SO}}}^{T_{\mathrm{SO}}} \left[\sum_{j=1}^{N} E_j(t - \tau_j)\right]^2 dt \tag{7}$$

by varying the time delays $\tau_j$. Given the different central frequencies of the component waveforms, the integrated intensity of the combined beam will remain roughly constant as time delays are varied, but by minimizing that intensity in some temporal region, we expect to generate superoscillatory behavior.

This objective function can be minimized in any number of ways, e.g., via gradient descent [56]. The cost function itself is nonconvex, meaning a number of local minima may be obtained depending on the initial guess for time delays. Note that while the minimization does not *guarantee* superoscillatory behavior, in practice we find that the time delays corresponding to minimizations of Eq. (7) uniformly result in superoscillations. Furthermore, any superoscillatory phenomenon involves a trade-off between the amplitude and frequency of the waveform, with higher effective frequencies having smaller amplitudes [15]. This means that the global minimum of the cost function is likely to correspond to a superoscillation whose amplitude is beyond the limit of experimental detection. It is therefore useful to have a number of minima when seeking the best balance between the amplitude and frequency of the superoscillation. As Fig. 3 demonstrates, there exist many minima corresponding to clearly superoscillatory waveforms that remain experimentally detectable.

*Experimental generation of superoscillations.*—As a first demonstration of the viability of this method for generating superoscillations, we experimentally combine four near-sinusoidal THz optical beams. In order to generate an optical time domain superoscillation in the THz regime, an amplified femtosecond laser centered at 1030 nm is employed. This has a pulse duration of 190 fs, 400 μJ pulse energy, and a 50 kHz repetition rate. This in turn is used to generate four near-sinusoidal waveforms $E_j(t)$, which have $f_j = 0.52, 0.63, 0.72, 0.82$ THz central frequencies. These waveforms are produced via optical rectification in periodically poled lithium niobate at room temperature (see Sec. I of [57]). This technique is widely used for generation of narrow band terahertz radiation [58–60].

After measuring each component waveform $E_j(t)$ individually (dashed lines on the left of Fig. 2), the minimization of Eq. (7) is performed. The time delays $\tau_j$ prescribed by this procedure are then implemented experimentally (solid lines on the left of Fig. 2). The right side of Fig. 2 shows the obtained experimental superoscillation that corresponds to one local minimum of the objective function, Eq. (7). This and two other local minima of Eq. (7) obtained in this process are shown in Fig. 3. As predicted, in each case superoscillations are clearly observed within the intensity-minimized region [Figs. 3(d)–3(f)]. These superoscillations are not only of a sufficient amplitude for detection, but exhibit excellent agreement with the theoretical prediction used to generate them.

The precise enhancement in frequency provided by the superoscillation may be quantified via a calculation of "local frequency." This is defined in analogy with the local wave number used to characterize spatial superoscillations [63], and is the gradient of the phase $f_{\mathrm{loc}} = (1/2\pi)(d\phi/dt)$. This is obtained by Hilbert transforming the real valued signal $E(t)$ into an analytic form [64] $\hat{E}(t)$, from which the field phase $\phi(t) = \arg \hat{E}(t)$ is extracted. As Figs. 3(g)–3(i) show, for most of the duration of the combined waveform, its local frequency is approximately equal to its highest frequency component. Within the region of minimization, however, the combined waveform's $f_{\mathrm{loc}}$ deviates sharply, experiencing a $\sim$2 fold increase relative to the highest frequency component.

*Superspectroscopy.*—Having generated superoscillatory fields, a natural question is how they may be profitably applied. An immediate application is to exploit their potential for off-resonance sensing to distinguish between spectroscopically similar substances, in a technique we term "superspectroscopy." To demonstrate this, we employ the same four time-limited $E_j(t)$ waveforms as the previous section, which we pass through samples of anhydrous $\alpha$-D-Glucose (glucose) or L-Glutamic acid (LGA) (for full details

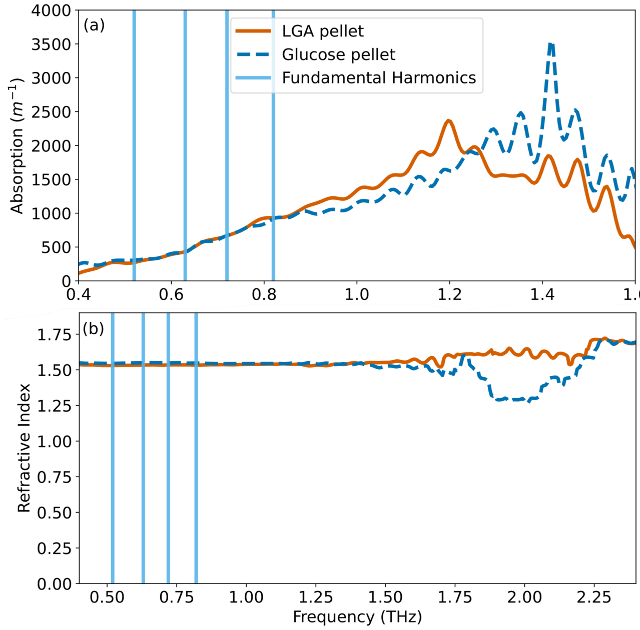


FIG. 4. The measured (a) absorption and (b) refractive index of our conventional THz time domain spectroscopy system for $\alpha$-d-Glucose and L-Glutamic Acid (LGA). The vertical lines indicate the four time-limited, quasisinusoidal waveforms of frequencies 0.52–0.82 THz that are combined to create the superoscillation. Within the region of the four source waveforms, the glucose and LGA samples have nearly identical absorption and refractive index.

see [57]). As Fig. 4 shows, both the absorption and refractive index of these materials are extremely similar within the range of frequencies of the constituent waveforms. To quantify the degree of distinguishability between the transmitted fields we define the dimensionless parameter $J$:

$$J = \frac{\int_{-T_{\mathrm{obs}}}^{T_{\mathrm{obs}}} [E_{\mathrm{Glu}}(t) - E_{\mathrm{LGA}}(t)]^2 dt}{\frac{1}{2}\int_{-T_{\mathrm{obs}}}^{T_{\mathrm{obs}}} [E_{\mathrm{Glu}}(t)^2 + E_{\mathrm{LGA}}(t)^2] dt}. \tag{8}$$

This measure characterizes the field difference averaged over some observational window (of size $2T_{\mathrm{obs}}$), normalized to the average intensity of the two responses (such that $J$ cannot be arbitrarily improved by uniformly increasing the amplitude of the incident fields).

Following the procedure outlined in Sec. II of [57], a set of time delays for the incident field [corresponding to some local minima of Eq. (7)] are chosen such that both $E_{\mathrm{Glu}}(t)$ and $E_{\mathrm{LGA}}(t)$ are superoscillatory in the region $t \in [-T_{\mathrm{SO}}, T_{\mathrm{SO}}]$, as shown in Fig. 5(a). From this, we measure the distinguishability $J$ as a function of $T_{\mathrm{obs}}$ for the superoscillatory responses, and compare this to the results obtained when driving each material using only a single frequency. As Fig. 5 demonstrates, the measured $J$ for the superoscillatory responses increases as the measurement region defined by $T_{\mathrm{obs}}$ becomes comparable to $T_{\mathrm{SO}}$. Comparing this $J$ to those

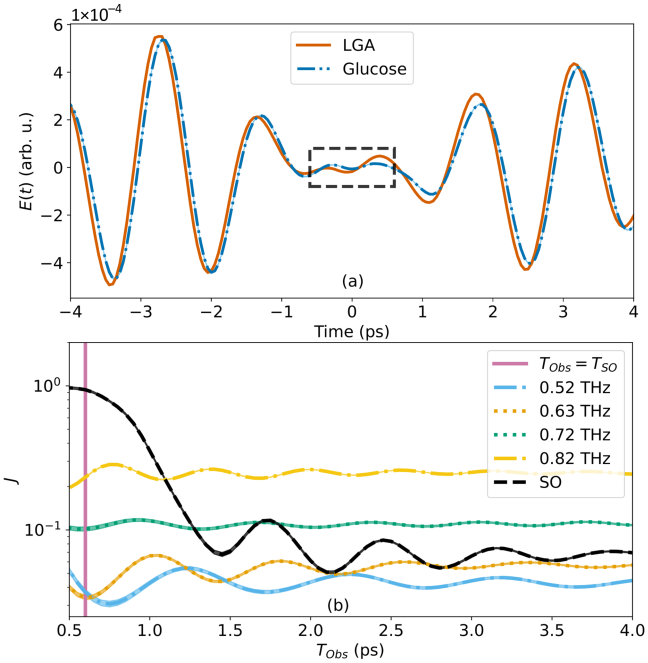


FIG. 5. (a) Measured transmitted waves of glucose and LGA pellets, with the region of superoscillation marked by a dashed black box. (b) Discriminability as a function of the observation window length $T_{\mathrm{obs}}$. The marked vertical line where $T_{\mathrm{obs}} = T_{\mathrm{SO}}$ indicates where the observational window matches the window of minimization. It is at this point $J$ is maximized for the superoscillatory driving, providing an enhancement of distinguishability of roughly an order of magnitude, as compared to measurements using individual source waveforms. In both panels shaded regions represent the 95% confidence limit, but on the scale represented this limit is in almost all cases within the thickness of the line plotted.

obtained driving with the individual component waveforms, we see that when $T_{\mathrm{obs}} \approx T_{\mathrm{SO}}$ the superoscillation produces a distinguishability enhancement of almost an order of magnitude relative to the 0.82 THz pulse.

*Outlook.*—The ability to probe systems with optical signals underpins the ongoing development of quantum technologies, and superoscillatory signals have the potential to greatly expand the tool set available to researchers. The present work addresses the question of how to practically generate such superoscillations in the time domain. While the results presented here employ a specific methodology for producing superoscillations, the ultimate goal of the method—to minimize pulse intensity over a given time window—can be achieved with a great variety of techniques. This freedom means that the prescription for generating superoscillations may be tailored to enforce some desired secondary properties, depending on the application and specific technique employed. Indeed, perhaps the principal future challenge will be to develop methodologies that maximize the control available in the generation of superoscillations. Nevertheless, as has been shown here, even a relatively simplistic prescription is capable of producing clearly detectable optical superoscillations in the time domain.

The potential applications of superoscillations cover a broad range of topics. Most obviously they extend the range of frequencies accessible by a given light source. This is of particular interest as researchers begin to explore dynamics in the attosecond regime [65]. At present the high frequency light necessary to probe this timescale is generated via highly nonlinear effects such as high harmonic generation [66–68], but superoscillations offer an alternative platform for realizing these light sources, without recourse to nonlinear effects.

Furthermore, recent developments in quantum control have demonstrated the highly malleable nature of driven systems, to the extent that one can force one material to “mimic” the optical response of another [69–72]. Such manipulations require complex, broadband fields, however, and superoscillations may facilitate the realization of these control fields.

Finally, we have also demonstrated a proof of concept for the advantage superoscillatory pulses can provide in distinguishing spectroscopically similar substances. In a follow-up work, we will determine how the choice of superoscillation in superspectroscopy can be optimized to further enhance distinguishability.

This work was supported by the W. M. Keck Foundation. D. I. B. and G. M. are also supported by Army Research Office (ARO) (Grant No. W911NF-23-1-0288; program manager Dr. James Joseph). The views and conclusions contained in this document are those of the authors and should not be interpreted as representing the official policies, either expressed or implied, of ARO or the U.S. Government. The U.S. Government is authorized to reproduce and distribute reprints for Government purposes notwithstanding any copyright notation herein.

*gmccaul@tulane.edu
†ppeng@tulane.edu
‡mortizmartinez@tulane.edu
§dlindberg@tulane.edu
‖dtalbaye@tulane.edu
¶dbondar@tulane.edu

[1] D. A. Lidar and S. Schneider, Stabilizing qubit coherence via tracking-control, Quantum Inf. Comput. **5** (2005).

[2] A. G. Campos, D. I. Bondar, R. Cabrera, and H. A. Rabitz, How to make distinct dynamical systems appear spectrally identical, Phys. Rev. Lett. **118**, 083201 (2017).

[3] P. Gross, H. Singh, H. Rabitz, K. Mease, and G. M. Huang, Inverse quantum-mechanical control: A means for design and a test of intuition, Phys. Rev. A **47**, 4593 (1993).

[4] Y. Chen, P. Gross, V. Ramakrishna, H. Rabitz, and K. Mease, Competitive tracking of molecular objectives described by quantum mechanics, J. Chem. Phys. **102**, 8001 (1995).

[5] Y. Chen, P. Gross, V. Ramakrishna, H. Rabitz, K. Mease, and H. Singh, Control of classical regime molecular objectives -applications of tracking and variations on the theme*, Automatica **33**, 1617 (1997).

[6] A. Magann, T.-S. Ho, and H. Rabitz, Singularity-free quantum tracking control of molecular rotor orientation, Phys. Rev. A **98**, 043429 (2018).

[7] G. McCaul, C. Orthodoxou, K. Jacobs, G. H. Booth, and D. I. Bondar, Driven imposters: Controlling expectations in many-body systems, Phys. Rev. Lett. **124**, 183201 (2020).

[8] G. McCaul, C. Orthodoxou, K. Jacobs, G. H. Booth, and D. I. Bondar, Controlling arbitrary observables in correlated many-body systems, Phys. Rev. A **101**, 053408 (2020).

[9] D. Pierangeli, G. Marcucci, and C. Conti, Photonic extreme learning machine by free-space optical propagation, Photonics Res. **9**, 1446 (2021).

[10] Y. Shen, N. C. Harris, S. Skirlo, M. Prabhu, T. Baehr-Jones, M. Hochberg, X. Sun, S. Zhao, H. Larochelle, D. Englund, and M. Soljacic, Deep learning with coherent nanophotonic circuits, Nat. Photonics **11**, 441 (2017).

[11] A. Opala, S. Ghosh, T. C. Liew, and M. Matuszewski, Neuromorphic computing in Ginzburg-Landau polariton-lattice systems, Phys. Rev. Appl. **11**, 064029 (2019).

[12] R. Hamerly, L. Bernstein, A. Sludds, M. Soljačić, and D. Englund, Large-scale optical neural networks based on photoelectric multiplication, Phys. Rev. X **9**, 021032 (2019).

[13] R. Pappu, B. Recht, J. Taylor, and N. Gershenfeld, Physical one-way functions, Science **297**, 2026 (2002).

[14] W. Bogaerts, D. Pérez, J. Capmany, D. A. Miller, J. Poon, D. Englund, F. Morichetti, and A. Melloni, Programmable photonic circuits, Nature (London) **586**, 207 (2020).

[15] M. Berry *et al.*, Roadmap on superoscillations, J. Opt. **21**, 053002 (2019).

[16] M. V. Berry, Faster than Fourier, in *Quantum Coherence and Reality; in Celebration of the 60th Birthday of Yakir Aharonov*, edited by J. S. Anandan and J. L. Safko (World Scientific, Singapore, 1994), pp. 55–65.

[17] K. S. Rogers and E. T. F. Rogers, Realising superoscillations: A review of mathematical tools and their application, J. Phys. **2**, 042004 (2020).

[18] Y. Aharonov, P. G. Bergmann, and J. L. Lebowitz, Time symmetry in the quantum process of measurement, Phys. Rev. **134**, B1410 (1964).

[19] Y. Aharonov, F. Colombo, I. Sabadini, D. C. Struppa, and J. Tollaksen, Some mathematical properties of superoscillations, J. Phys. A **44**, 365304 (2011).

[20] Y. Aharonov, F. Colombo, I. Sabadini, D. C. Struppa, and J. Tollaksen, On some operators associated to superoscillations, Complex Anal. Oper. Theor. **7**, 1299 (2013).

[21] Y. Aharonov, E. Ben-Reuven, S. Popescu, and D. Rohrlich, Perturbative induction of vector potentials, Phys. Rev. Lett. **65**, 3065 (1990).

[22] N. I. Zheludev and G. Yuan, Optical superoscillation technologies beyond the diffraction limit, Nat. Rev. Phys. **4**, 16 (2021).

[23] G. H. Yuan and N. I. Zheludev, Detecting nanometric displacements with optical ruler metrology, Science **364**, 771 (2019).

[24] M. V. Berry and S. Popescu, Evolution of quantum superoscillations and optical superresolution without evanescent waves, J. Phys. A **39**, 6965 (2006).

[25] J. Lindberg, Mathematical concepts of optical superresolution, J. Opt. A **14**, 083001 (2012).

[26] M. V. Berry and S. Popescu, Evolution of quantum superoscillations and optical superresolution without evanescent waves, J. Phys. A **39**, 6965 (2006).

[27] Y. Eliezer and A. Bahabad, Super-transmission: The delivery of superoscillations through the absorbing resonance of a dielectric medium, Opt. Express **22**, 31212 (2014).

[28] J. H. Eberly, Correlation, coherence and context, Laser Phys. **26**, 084004 (2016).

[29] S. Zarkovsky, Y. Ben-Ezra, and M. Schwartz, Transmission of Superoscillations, Sci. Rep. **10**, 5893 (2020).

[30] G. Yuan, E. T. F. Rogers, and N. I. Zheludev, "Plasmonics" in free space: Observation of giant wavevectors, vortices, and energy backflow in superoscillatory optical fields, Light **8**, 2 (2019).

[31] F. M. Huang and N. I. Zheludev, Super-resolution without evanescent waves, Nano Lett. **9**, 1249 (2009).

[32] E. T. F. Rogers, J. Lindberg, T. Roy, S. Savo, J. E. Chad, M. R. Dennis, and N. I. Zheludev, A super-oscillatory lens optical microscope for subwavelength imaging, Nat. Mater. **11**, 432 (2012).

[33] S. Legaria, J. Teniente, S. Kuznetsov, V. Pacheco-Peña, and M. Beruete, Highly efficient focusing of terahertz waves with an ultrathin superoscillatory metalens: Experimental demonstration, Adv. Photonics Res. **2**, 2000165 (2021).

[34] T. Pu, J.-Y. Ou, V. Savinov, G. Yuan, N. Papasimakis, and N. I. Zheludev, Unlabeled far-field deeply subwavelength topological microscopy (dstm), Adv. Sci. **8**, 2002886 (2021).

[35] S. Legaria, V. Pacheco-Peña, and M. Beruete, Superoscillatory metalens at terahertz for enhanced focusing with reduced side lobes, Photonics **5**, 56 (2018).

[36] A. M. H. Wong and G. V. Eleftheriades, Temporal pulse compression beyond the Fourier transform limit, IEEE Trans. Microwave Theory Tech. **59**, 2173 (2011).

[37] A. M. H. Wong and G. V. Eleftheriades, Superoscillatory radar imaging: Improving radar range resolution beyond fundamental bandwidth limitations, IEEE Microwave Wireless Compon. Lett. **22**, 147 (2012).

[38] S. Brehm, A. V. Akimov, R. P. Campion, and A. J. Kent, Temporal superoscillations of subterahertz coherent acoustic phonons, Phys. Rev. Res. **2**, 023009 (2020).

[39] Y. Eliezer, L. Hareli, L. Lobachinsky, S. Froim, and A. Bahabad, Breaking the temporal resolution limit by superoscillating optical beats, Phys. Rev. Lett. **119**, 043903 (2017).

[40] Y. Eliezer, B. K. Singh, L. Hareli, A. bahabad, and A. Arie, Experimental realization of structured super-oscillatory pulses, Opt. Express **26**, 4933 (2018).

[41] E. G. Neyra, G. A. Torchia, P. Vaveliuk, and F. Videla, Simple interferometric setup enabling sub-Fourier-scale ultra-short laser pulses, J. Opt. **24**, 045504 (2022).

[42] F. A. Hegmann and M. S. Sherwin, Generation of picosecond far-infrared pulses using laser-activated semiconductor reflection switches, in *Millimeter and Submillimeter Waves and Applications III*, edited by M. N. Afsar,

International Society for Optics and Photonics (SPIE, Denver Colorado, 1996), Vol. 2842, pp. 90–105.
[43] F. A. Hegmann, J. B. Williams, B. Cole, M. S. Sherwin, J. W. Beeman, and E. E. Haller, Time-resolved photoresponse of a gallium-doped germanium photoconductor using a variable pulse-width terahertz source, Appl. Phys. Lett. **76**, 262 (2000).
[44] M. F. Doty, B. E. Cole, B. T. King, and M. S. Sherwin, Wavelength-specific laser-activated switches for improved contrast ratio in generation of short thz pulses, Rev. Sci. Instrum. **75**, 2921 (2004).
[45] J. Bühler, J. Allerbeck, G. Fitzky, D. Brida, and A. Leitenstorfer, Terahertz shockwaves generated by a precise subcycle cut of the electric field, Optica **5**, 821 (2018).
[46] G. H. Yuan, E. T. Rogers, and N. I. Zheludev, Achromatic super-oscillatory lenses with sub-wavelength focusing, Light Sci. Appl. **6**, e17036 (2017).
[47] M. V. Berry, Suppression of superoscillations by noise, J. Phys. A **50**, 025003 (2016).
[48] E. Tang, L. Garg, and A. Kempf, Scaling properties of superoscillations and the extension to periodic signals, J. Phys. A **49**, 335202 (2016).
[49] E. Katzav, E. Perlsman, and M. Schwartz, Yield statistics of interpolated superoscillations, J. Phys. A **50**, 025001 (2016).
[50] Y. Kozawa, D. Matsunaga, and S. Sato, Superresolution imaging via superoscillation focusing of a radially polarized beam, Optica **5**, 86 (2018).
[51] S. S. Stafeev, A. G. Nalimov, M. V. Kotlyar, D. Gibson, S. Song, L. O'Faolain, and V. V. Kotlyar, Microlens-aided focusing of linearly and azimuthally polarized laser light, Opt. Express **24**, 29800 (2016).
[52] J. Ahn, A. V. Efimov, R. D. Averitt, and A. J. Taylor, Terahertz waveform synthesis via optical rectification of shaped ultrafast laser pulses, Opt. Express **11**, 2486 (2003).
[53] L. Gingras and D. G. Cooke, Direct temporal shaping of terahertz light pulses, Optica **4**, 1416 (2017).
[54] M. Veli, D. Mengu, N. T. Yardimci, Y. Luo, J. Li, Y. Rivenson, M. Jarrahi, and A. Ozcan, Terahertz pulse shaping using diffractive surfaces, Nat. Commun. **12**, 37 (2021).
[55] A. Herter, A. Shams-Ansari, F. F. Settembrini, H. K. Warner, J. Faist, M. Lončar, and I.-C. Benea-Chelmus, Terahertz waveform synthesis in integrated thin-film lithium niobate platform, Nat. Commun. **14**, 11 (2023).
[56] R. Fletcher, *Practical Methods of Optimization* (Wiley, Chichester, 2000).
[57] See Supplemental Material at http://link.aps.org/supplemental/10.1103/PhysRevLett.131.153803 for a detailed description of the experimental setup and demonstration of superspectroscopy, which includes Refs. [58–62].
[58] A. Nahata, A. S. Weling, and T. F. Heinz, A wideband coherent terahertz spectroscopy system using optical rectification and electrooptic sampling, Appl. Phys. Lett. **69**, 2321 (1996).
[59] C. Weiss, G. Torosyan, J.-P. Meyn, R. Wallenstein, R. Beigang, and Y. Avetisyan, Tuning characteristics of narrowband thz radiation generated via optical rectification in periodically poled lithium niobate, Opt. Express **8**, 497 (2001).
[60] Y.-S. Lee, T. Meade, V. Perlin, H. Winful, T. B. Norris, and A. Galvanauskas, Generation of narrow-band terahertz radiation via optical rectification of femtosecond pulses in periodically poled lithium niobate, Appl. Phys. Lett. **76**, 2505 (2000).
[61] Q. Wu and X. Zhang, Freespace electrooptic sampling of terahertz beams, Appl. Phys. Lett. **67**, 3523 (1995).
[62] Q. Wu, M. Litz, and X. Zhang, Broadband detection capability of znte electrooptic field detectors, Appl. Phys. Lett. **68**, 2924 (1996).
[63] E. T. F. Rogers and N. I. Zheludev, Optical super-oscillations: Sub-wavelength light focusing and super-resolution imaging, J. Opt. **15**, 094008 (2013).
[64] J. Smith, *Mathematics of the Discrete Fourier Transform (DFT): With Audio Applications* (BookSurge Publishing, Seattle, WA, 2007), https://www.booksurge.com.
[65] F. Krausz and M. Ivanov, Attosecond physics, Rev. Mod. Phys. **81**, 163 (2009).
[66] S. Ghimire, A. D. DiChiara, E. Sistrunk, U. B. Szafruga, P. Agostini, L. F. DiMauro, and D. A. Reis, Redshift in the optical absorption of ZnO single crystals in the presence of an intense midinfrared laser field, Phys. Rev. Lett. **107**, 167407 (2011).
[67] S. Ghimire, A. D. DiChiara, E. Sistrunk, G. Ndabashimiye, U. B. Szafruga, A. Mohammad, P. Agostini, L. F. Dimauro, and D. A. Reis, Generation and propagation of high-order harmonics in crystals, Phys. Rev. A **85**, 043836 (2012).
[68] R. E. Silva, I. V. Blinov, A. N. Rubtsov, O. Smirnova, and M. Ivanov, High-harmonic spectroscopy of ultrafast many-body dynamics in strongly correlated systems, Nat. Photonics **12**, 266 (2018).
[69] A. G. Campos, D. I. Bondar, R. Cabrera, and H. A. Rabitz, How to make distinct dynamical systems appear spectrally identical, Phys. Rev. Lett. **118**, 083201 (2017).
[70] P. Ball, Masters of disguise, Nat. Mater. **19**, 710 (2020).
[71] G. McCaul, A. F. King, and D. I. Bondar, Optical indistinguishability via twinning fields, Phys. Rev. Lett. **127**, 113201 (2021).
[72] A. B. Magann, G. McCaul, H. A. Rabitz, and D. I. Bondar, Sequential optical response suppression for chemical mixture characterization, Quantum **6**, 626 (2022).